# Ferromagnetic resonance in Mn 5 Ge 3 epitaxial films with weak stripe domain structure

R Kalvig, E Jedryka, P. Aleshkevych, M Wojcik, W Bednarski, Matthieu Petit, L. Michez

# Ferromagnetic resonance in $Mn_5Ge_3$ epitaxial films with weak stripe domain structure

R. Kalvig,[1] E. Jedryka,[1] P. Aleshkevych,[1] M. Wojcik,[1] W. Bednarski,[2] M. Petit,[3] and L. Michez[3]

[1] *Institute of Physics, Polish Academy of Sciences, Aleja Lotników 32/46, PL–02668 Warsaw, Poland*

[2] *Institute of Molecular Physics, Polish Academy of Sciences, ul. Mariana Smoluchowskiego 17, 60-179 Poznań, Poland*

[3] *Aix-Marseille Université, CNRS, CINaM UMR 7325, 13288 Marseille, France*

Extensive X–band and Q–band FMR experiments have been performed in the $Mn_5Ge_3$ epitaxial films with thicknesses varying between 4.5 and 68 nm. FMR signals were recorded in the temperature range between 15 and 295 K, at different orientations of magnetic field with respect to the film plane. In addition to the acoustic FMR mode with well defined resonance field, originating from inside the magnetic domains, a broad absorption line has been observed at low fields and attributed to the unresolved spectrum of FMR modes having the origin in flux closure caps. The FMR results have been discussed in the context of the domain structure computed with the use of OOMMF micromagnetic calculations and giving good agreement with the experimental hysteresis curves. From the Q–band experiments, where the FMR signal is observed in magnetically saturated sample, the uniaxial anisotropy constant in films with different thicknesses has been determined as a function of temperature. This FMR study provides the evidence that the strong uniaxial anisotropy observed in epitaxial thin films of $Mn_5Ge_3$ leads to the formation of a stripe domain structure above 25 nm, in agreement with the published reports on magnetization studies in these films. It also eliminates a possible confusion that may arise from previously published FMR studies on films grown with the same method, which led their authors to conclude that the shape anisotropy can force the magnetization to the in–plane orientaion in this thickness range and even above it.

## I. INTRODUCTION

Ferromagnetic compound $Mn_5Ge_3$ is of interest for spintronic applications, due to considerable spin polarization (42%) and high Curie temperature (296 K) which can be further increased (up to 445 K) by the addition of carbon [1, 2]. Importantly, this compound is compatible with the mainstream silicon technology and can be epitaxially grown on Ge, maintaining its magnetic properties and metallic conductivity [3, 4]. Moreover, it displays strong magnetocrystalline anisotropy with hexagonal c–axis as an easy direction, which makes it prospective for spintronic and magnetic recording applications [5].

It has been shown that this compound can be successfully grown by Solid Phase Epitaxy (SPE), consisting in a room temperature Mn deposition on the Ge(111) substrate followed by thermal annealing. Good quality epitaxial films can be obtained with (0001) hexagonal c–axis parallel to the Ge(111) direction [6]. A detailed analysis of magnetization reversal process in the SPE–prepared thin films of $Mn_5Ge_3$ revealed that in the thickness range between 10 nm and 20 nm, magnetization direction at low temperatures undergoes reorientation from the in–plane to out–of–plane direction (i.e. along the hexagonal c–axis) and at 25 nm a clear signature of a multi–domain structure with perpendicular orientation was observed [5, 7].

Meanwhile, another study in $Mn_5Ge_3$ films prepared with the same technique [8], has reported–based on the analysis of Ferromagnetic Resonance (FMR) experiments–that in spite of the demonstrated uniaxial anisotropy perpendicular to the film plane, magnetization is oriented in sample plane, within the investigated range of temperatures (30–290 K), even in samples as thick as 30 nm. This evident discrepancy requires a closer examination, especially since the FMR experiments reported in [8] were performed at 9.08 GHz (X-band), and the corresponding FMR signals were observed at magnetic field values below sample saturation, therefore some kind of domain structure can be expected. To resolve these discrepancies and to get a deeper insight into the magnetic properties of epitaxial thin films prepared by SPE method, we have undertaken an extensive FMR study in the Q–band, where the FMR resonance takes place in a fully saturated sample, as well as in the X–band (in presence of a domain structure). $Mn_5Ge_3$ films with thicknesses varying between 4.5 and 68 nm have been studied as a function of temperature and sample orientation. Our results show unambiguously that in the investigated film thickness range between 18 and 68 nm the uniaxial anisotropy prevails over the shape anisotropy leading to the stripe domain structure with closure caps containing a significant fraction of magnetic moments.

Analysis of our FMR data, supported by a simulation of the magnetic moments distribution using the OOMMF software package [9], made it possible to identify particular fragments of the domain structure giving rise to the resonance modes observed at X–band: on one hand an acoustic FMR mode with well–defined resonance field originating from magnetization inside the stripe domains, and on the other hand–a broad absorption spectrum observed at low fields, attributed to flux closure caps. The Q–band experiments, where the uniform precession mode is observed in magnetically saturated sample, made it possible to determine the uniaxial anisotropy constant

as a function of temperature in films with different thicknesses.

## II. EXPERIMENTAL DETAILS

Thin films of $Mn_5Ge_3$ with thickness of 4.5 nm, 9 nm, 18 nm and 68 nm have been prepared on the Ge(111) substrates (500 $\mu$m thick) by solid phase epitaxy (SPE) in molecular beam epitaxy (MBE) chamber with a base pressure less than $10^{-10}$ Torr. The SPE preparation consists of a room temperature deposition of Mn layer followed by thermal annealing at 720 K to activate interdiffusion between the deposited metal and the germanium buffer layer. The as prepared $Mn_5Ge_3$ films have been capped with amorphous Ge to prevent oxidation. Further details on sample preparation are given in ref [6, 10]. The quality of crystal growth has been monitored *in situ* using reflection high–energy electron diffraction (RHEED). The obtained samples have been characterized by XRD technique–the scan clearly indicates two narrow reflections (0002) and (0004) evidencing good quality $Mn_5Ge_3$ phase. The XRD results confirm also that c–axis of $Mn_5Ge_3$ is parallel to Ge(111) [7].

Magnetic characterization was performed using a Quantum Design superconducting quantum interference device magnetometer (SQUID). In order to understand better the magnetic properties and the evolution of a domain structure postulated from these measurements, micromagnetic simulations of the magnetic moment distribution within the sample have been performed with the use of the OOMMF software package [9] and compared with the experimental data.

Ferromagnetic resonance experiments at X–band (9.38 GHz) were performed by means of a commercial Bruker EMX electron spin resonance spectrometer with a rectangular microwave cavity working in the $TE_{102}$ mode and a standard phase sensitive detection. External magnetic field was modulated at 100 kHz. The temperature has been varied in the range 15–295 K with the use of an Oxford helium–flow cryostat. The samples were mounted on a quartz holder and the measurements were performed with magnetic field applied in the plane of a sample and perpendicular to it, whereas microwave field was applied parallel to the sample plane and perpendicular to the DC bias field. Due to a strong uniaxial anisotropy of the studied compounds, the resonance field in parallel orientation of the DC magnetic field was below the saturation field in the X–band, therefore additional measurements have been performed in the Q–band (34 GHz) with the use of BrukerElexSys E500 spectrometer equipped with flexline ER 50106QT/W resonator and ER 4118CF cryostat operating at 3.8–295 K. Temperature was controlled and stabilized with the Oxford Instruments temperature controller ITC 503S. FMR spectra were recorded as the first derivative of the microwave power (about 2 mW) absorption versus the external magnetic field in the range of 0–17 kOe. Magnetic field was modulated with the frequency of 100 kHz and modulation amplitude of the order of 10 Oe. The respective configuration of the pumping field versus DC bias magnetic field was the same as in case of the X–band experiment. Manual homemade goniometer was used in the studies of angular dependences of the resonance fields.

## III. RESULTS AND DISCUSSION

### A. Magnetization reversal and micromagnetic OOMMF simulations of the domain structure

A thorough study of magnetization reversal at low temperatures in $Mn_5Ge_3$ thin films used in this study has been reported in Ref. [5, 7], as a function of film thickness. In case of magnetic field applied in the film plane, hysteresis loops recorded in very thin films have a square shape indicating that the magnetization follows the external field, and above 16 nm the loops become canted. As an example, in Fig. 1 we present the magnetic hysteresis loop measured at 15 K in 25 nm film. Magnetization reaches its saturation value of 1450 emu/cm$^3$ for the in–plane fields higher than 6.3 kOe. We also note a coercive field of 500 Oe and remanence magnetization corresponding to about 20% of saturation value, indicating the presence of an in–plane component of magnetization. In the same figure we plot the theoretical curve computed for a 30 nm thick film using the OOMMF package, as described below.

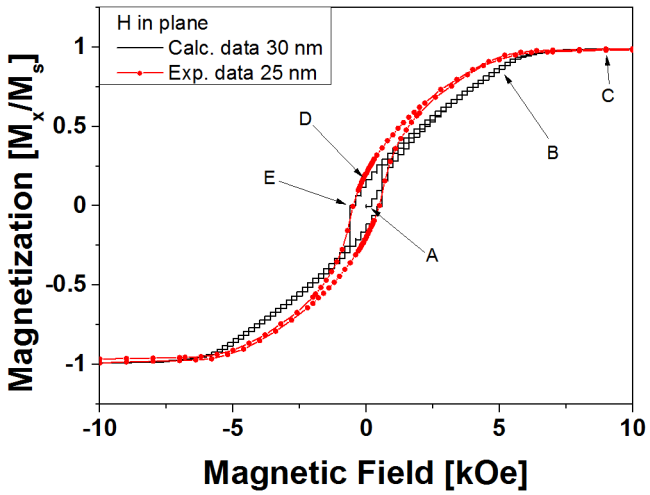


FIG. 1. (Color online) Solid–dotted line: experimental hysteresis loop recorded with SQUID magnetometer at 15 K in $Mn_5Ge_3$ epitaxial film (25 nm), with magnetic field swept in the film plane. Solid line: theoretical curve computed with the use of OOMMF software. Letters A–E indicate characteristic points giving rise to the domain structure presented in diagrams in Fig. 3.

Magnetization curves recorded from the same sample with magnetic field applied perpendicular to the film plane, are shown in Fig. 2. Magnetic saturation in the out–of–plane configuration is reached around 10.3 kOe.

With decreasing magnetic field the system reveals an inertia: magnetization maintains its saturation value, and then at around 8.1 kOe it suddenly drops down. This is a well-known effect due to the fact that the oppositely magnetized domain has to reach a certain minimum dimension in order to create a stable domain configuration. Therefore the magnetization curve in the "field–down" direction does not follow the same values as in the "field–up" direction, creating a small loop just below the saturation field. This loop is better visible in the thicker samples, as shown in Fig. 2 inset, where we present the blow–up of the high field detail of the hysteresis loop recorded from the 68 nm thick film (note that the bubble nucleation region in case of 68 nm film is between 9.1 and 9.7 kOe). The curves corresponding to other films from the same series of samples, revealing the small loop feature, have been presented in the Fig. 3 of Ref. [5]. Similar small loops have also been reported in other films with stripe domain structure, e.g. (0001)–hcp cobalt films [11] or thin films of $Co_2MnGa$ Heusler alloy [12].

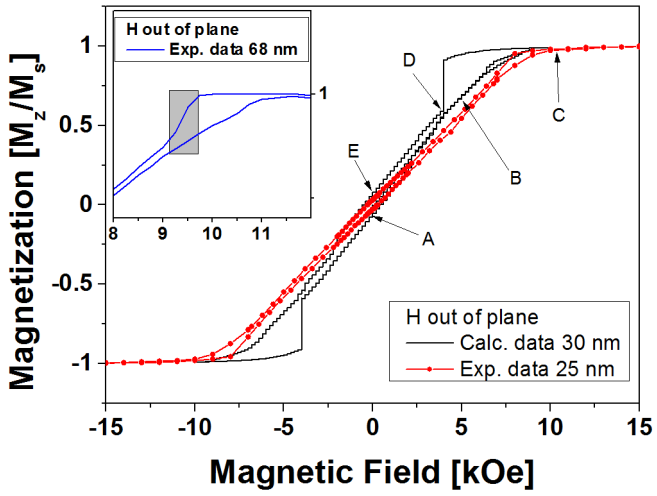


FIG. 2. (Color online) Solid–dotted line: experimental hysteresis loop recorded with SQUID magnetometer at 15 K in $Mn_5Ge_3$ epitaxial film (25 nm), with magnetic field swept out–of–plane. Solid line: theoretical curve computed with the use of OOMMF software. Letters A–E indicate characteristic points giving rise to the domain structure presented in diagrams in Fig. 4. The inset shows the blow–up of the high–field section of the experimental curve for 68 nm thick sample, indicating the field region corresponding to bubble nucleation.

The material parameters obtained from magnetization studies were used in Ref. [7] to determine the ratio between the uniaxial perpendicular magnetocrystalline anisotropy and the shape anisotropy of the thin film, described by the so called quality factor, defined as $Q=K_u/(2\pi M_s^2)$, which was found in the studied materials to be around 0.6 at 15 K [7]. Thin films of the low Q–factor materials ($Q<1$), do not develop an open stripe domain structure, as is the case of materials with $Q>1$, but rather tend to form a flux closure caps at the film surface. Therefore in addition to the wide Bloch–type domain walls within the film volume, one can expect at the film surface a fraction of magnetic moments with the in–plane orientation, separated by the Neel–type domain walls. Interpretation of the FMR data in such a complex domain structure requires a detailed consideration of magnetic moment distribution. To this end, we performed micromagnetic calculations with the use of freely available software package OOMMF [9]. Simulated volume was a cuboid with dimensions 150 nm x 150 nm x 30 nm, whereas the discretization cell was cube of side 1.5 nm. Exchange stiffness parameter A was taken as $A=1\cdot10^{-7}$ erg/cm from Ref. [5] and uniaxial anisotropy constant $K_u=5.66\cdot10^6$ erg/cm$^3$ was taken from the Q–band FMR experiment as described in the next section. Saturation magnetization was estimated as 1450 emu/cm$^3$, based on the experimental hysteresis loops. Calculations were carried out by minimizing the total energy in each discretization cell, while the external magnetic field was applied with 200 Oe step, from 0 field to 10 kOe in sample plane (direction x on Fig. 3), and then in the opposite direction (–x) to –10 kOe and back to 10 kOe. Similar procedure was applied for magnetic field perpendicular to sample plane (along z–axis).

Magnetic hysteresis loops computed in the in–plane and out–of–plane configuration reproduce correctly the features of experimental curves, as shown in Fig. 1 and Fig. 2, respectively. The magnetization curve calculated for field applied in sample plane (Fig. 1) is almost identical to the experimental data, with saturation field around 6.3 kOe and remanence magnetization of about 20% of saturation value. The curve computed for field oriented perpendicular to sample plane reveals a different value of domain nucleation field and much broader loops around saturation than the experimental data recorded for 25 nm film. This is probably due to the fact that in a real material there may be a certain distribution of demagnetizing fields due to the miniscule variations in surface roughness and to the influence of a capping layer. Nevertheless, the general character of the magnetization reversal is reproduced, proving that the calculated magnetic structure represents closely the magnetic moment distribution in a real material.

Fig. 3 and Fig. 4 visualizes the magnetic domain structure resulting from the micromagnetic calculations, as a function of magnetic field applied along the x–axis and z–axis, respectively (the coordinate system used is shown in panels A). The respective panel columns visualize the magnetic moment distribution in 30 nm $Mn_5Ge_3$ film in the three projections: (1) Top view at sample surface, (2) x–y cross section at half–thickness and (3) y–z cross section. The rows A, B, C, D, E correspond to characteristic field values, as indicated on the hysteresis loops in Fig. 1 and Fig. 2. Point A in Fig. 1 corresponds to initial magnetic equilibrium state in this material before turning the magnetic field on. In panels A of Fig. 3 we note a clearly visible domain structure with two oppositely oriented domains, up and down along the c–axis separated by the Bloch–type walls. White color and blue

arrows indicate magnetic moments pointing in the "+z" direction (domains "up"), whereas black color and red arrows describe domains oriented "down" in the "–z" direction. Green background and black arrows represent fractions of the sample volume where magnetic moments are oriented in sample plane. Flux closure caps on the film surface as well as Bloch wall centers in the sample volume are the main contributors to the in–plane magnetization (remanence around zero field). With increasing in–plane field value, i.e. going towards point B in Fig. 1, the magnetization inside domains tilts towards the field direction, forming a characteristic stripe domain pattern, until a full saturation in the film plane (point C) is reached. Upon subsequent decreasing the field value, the stripe domain pattern is recovered and it is preserved when the field is switched off (point D). Application of magnetic field in the opposite direction reverts the spins on the surface as shown in the panel E1 in Fig. 3, and magnetic moments inside the domains also begin to tilt towards the "–x" direction.

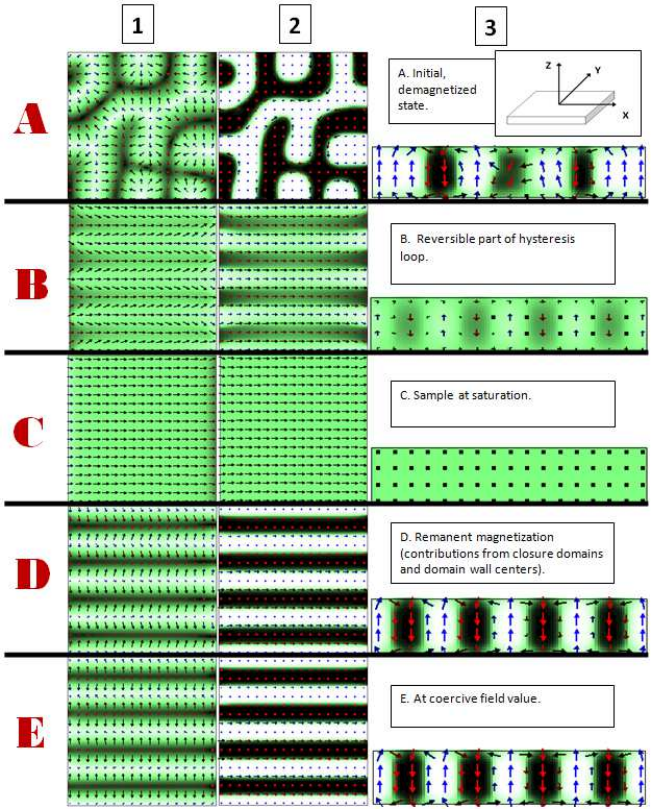


FIG. 3. (Color online) Diagrams showing magnetic moment distribution in different parts of 30 nm $Mn_5Ge_3$ film, computed with the use of OOMMF software package. Magnetic field applied in the film plane, rows (A,B,...E) correspond to characteristic points of hysteresis loop in Fig. 1. Columns represent different projections: [1]: Top view at sample surface, [2]: x–y cross section at half–thickness and [3]: y–z cross section. For details see the text.

The evolution of a domain structure in case of magnetic field applied in the direction perpendicular to the film is illustrated in Fig. 4, using the same convention of colors. Starting from the same domain pattern (panel A), which corresponds to the initial point A, we observe a progressive shrinking of the domains with magnetization oriented opposite to the applied field. At point B (5 kOe) only two cylindrical domains with magnetization in the "–z" direction remain, and at point C the sample is fully saturated in the "+z" direction. Point D is the characteristic point on the hysteresis curve where a sudden drop of magnetization from its saturation value takes place. At this field value we note the onset of a number of well–defined bubble domains magnetized in "–z" direction (panel D). Finally, at point E, in the absence of magnetic field, the equilibrium between "up" and "down" domains is recovered.

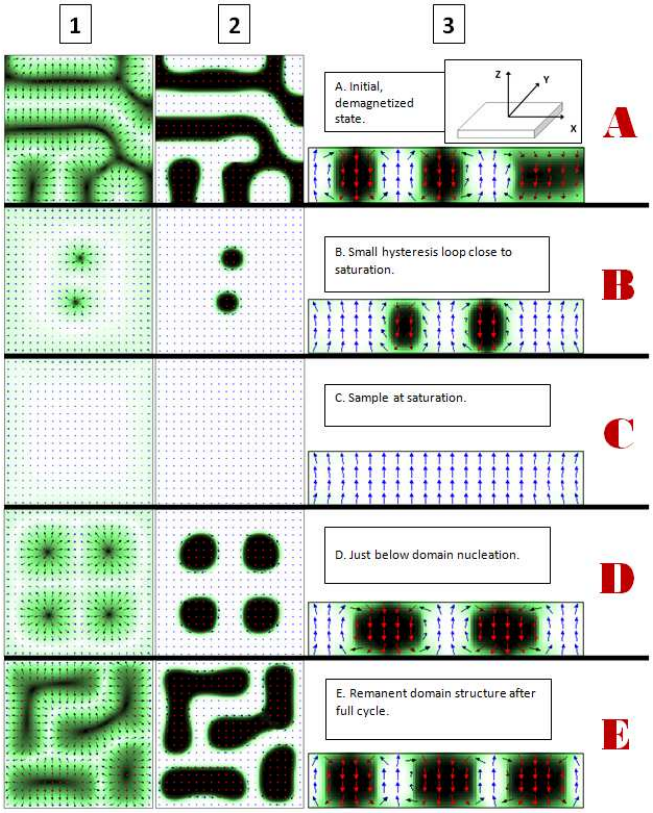


FIG. 4. (Color online) Diagrams showing magnetic moment distribution in different parts of 30 nm $Mn_5Ge_3$ film, computed with the use of OOMMF software package. Magnetic field applied perpendicular to the film plane, rows (A,B,...E) correspond to characteristic points of hysteresis loop in Fig. 2. Columns represent different projections: [1]: Top view at sample surface, [2]: x–y cross section at half–thickness and [3]: y–z cross section. For details see the text.

In conclusion, the micromagnetic calculations performed in $Mn_5Ge_3$ films with thickness of 30 nm reproduce correctly the experimental magnetization curves and provide the evidence for presence of a stripe domain structure typical for the low Q–factor materials, at least above 25 nm. Considering the systematic evolution of hysteresis curves as a function of film thickness reported in Ref. [5] one can extend this conclusion at least up to the thickest sample in this study (68 nm) where regular

stripe domain structure is expected.

### B. FMR studies

Fig. 5 presents the absorption derivative X–band FMR spectra recorded at 100 K from films with thicknesses between 4.5 and 68 nm, for the two orientations of DC magnetic field: in the film plane and perpendicular to it. All the films reveal two characteristic spectrum components: a narrow, well resolved resonance line and a very broad absorption signal at low field values. In case of 4.5 nm film this broad signal represents almost entire spectrum intensity, the narrow mode is merely marked.

A remarkable observation is that in case of 68 nm sample, the narrow FMR signal in the out–of–plane configuration could only be observed when the magnetic field was swept downwards after the sample was saturated in the out–of–plane direction. When starting from a demagnetized state and increasing the field all the way up to saturation, only the broad absorption at low fields was recorded, as shown in Fig. 6 where we present the X–band FMR spectra recorded in this sample at different temperatures, while sweeping the field upwards (red dashed line) and downwards (black line).

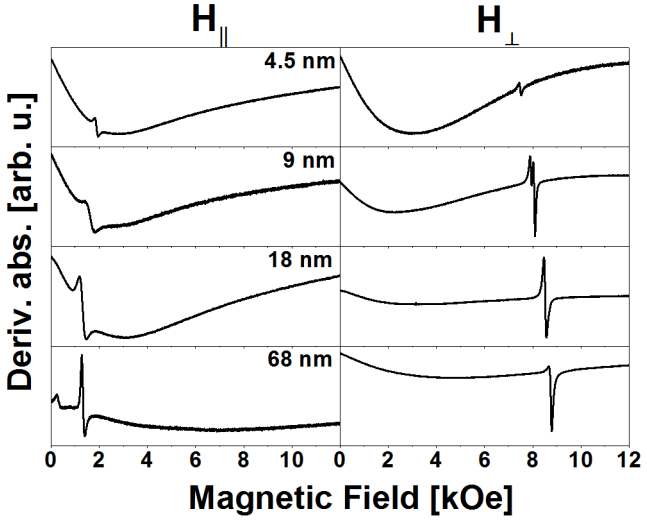


FIG. 5. Absorption derivative FMR spectra recorded from $Mn_5Ge_3$ films with thickness between 4.5 nm and 68 nm. The experiment was performed at X–band (9.38 GHz) at 100 K with DC field applied parallel (left) and perpendicular (right) to the film plane.

To understand better the origin of the observed FMR signals, we performed additional experiments at 34 GHz (Q–band). The absorption derivative FMR spectra recorded at different temperatures from the same 68 nm thick $Mn_5Ge_3$ film at Q–band are presented in Fig. 7. Similar to the X–band experiments, the spectra recorded at Q–band consist of a narrow, well resolved resonance line and a very broad absorption signal at low field values. In case of Q–band experiment with the DC field applied

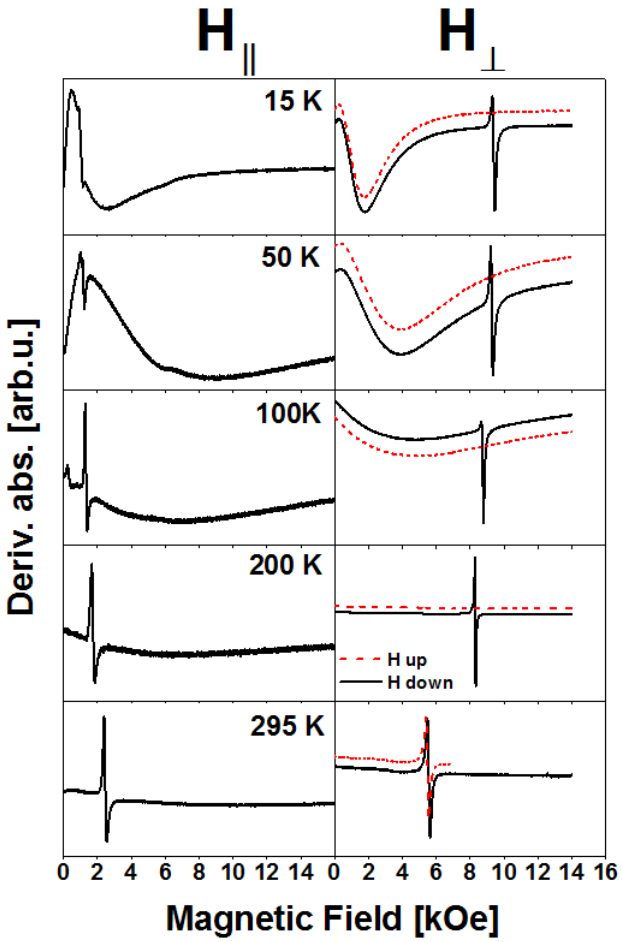


FIG. 6. (Color online) Absorption derivative FMR spectra recorded from the 68 nm thick $Mn_5Ge_3$ film at X–band (9.38 GHz) at temperatures between 15 K and 295 K. Left column: magnetic field applied in the film plane, right: magnetic field applied perpendicular to the film plane. Red dashed line (shifted along y axis to ensure visibility): sweeping upwards the magnetic field (note the absence of narrow FMR mode); black line: sweep–down. For details see the text.

perpendicular to the film plane, the resonance field of the narrow line in 68 nm sample is beyond the available field range at low temperatures–it could however be retrieved at 295 K, as shown in Fig. 7.

To identify the origin of the narrow resonance mode it is useful to consider the position of the resonance field as a function of film thickness. Fig. 8 summarizes the resonance field values of the well resolved FMR line (X–band and Q–band experiment) in case of the external magnetic field oriented in–plane and out–of–plane at 15 K. It also shows the respective saturation field values determined from the magnetization measurements. Vertical dashed lines separate three thickness regions where magnetization reversal studies indicate its equilibrium orientation in the film plane (below 10 nm), perpendicular to it (above 20 nm), and the reorientation region in–between [7].

It is well established that the FMR spectra in thin

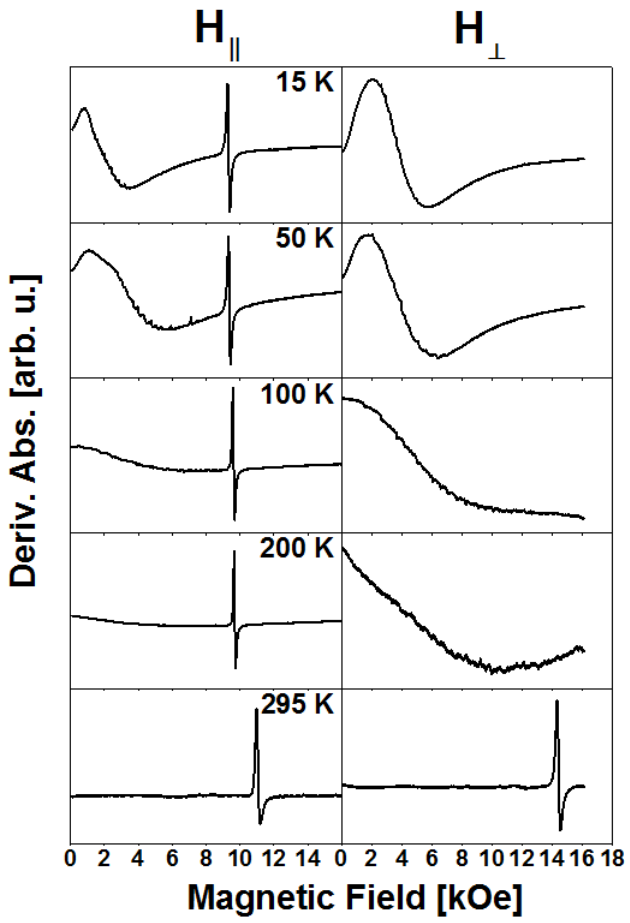


FIG. 7. Absorption derivative FMR spectra recorded from the 68 nm thick $Mn_5Ge_3$ film at Q–band (34 GHz) at temperatures between 15 K and 295 K. Left column: magnetic field applied in the film plane, right: magnetic field applied perpendicular to the film plane.

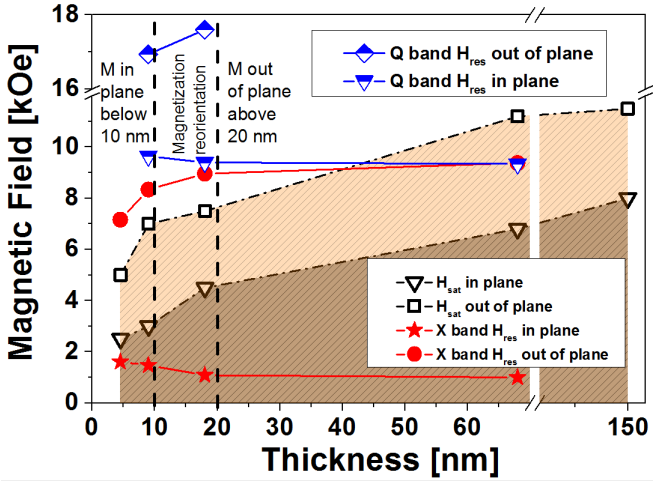


FIG. 8. (Color online) Magnetic saturation field values (in–plane and out–of–plane) and the respective resonance field values in the X–band and Q–band FMR experiment at 15 K, as a function of film thickness. Vertical dashed lines indicated the magnetization reorientation region reported in Ref. [7].

magnetic films with stripe domains can have a complex structure, consisting of a number of resonance modes. In the simplest case of high–Q material, the resonances in the adjacent "up" and "down" domains, separated by the Bloch walls, are coupled via the dipolar demagnetization fields, splitting the FMR signal in two branches: in–phase mode $\omega^+$(denoted also as acoustic) and out–of–phase $\omega^-$ mode (optical), the latter observed at higher field values [13, 14]. Theoretical calculations of Vukadinovic et al. [15] have shown the dependence of the $\omega^+$ and $\omega^-$ frequencies in high–Q materials on magnetic parameters such as quality factor, demagnetization, and damping parameter, giving a satisfactory agreement with the experimental results on bismuth–substituted single crystal garnet films. In addition to these two basic FMR modes a third absorption mode, due to resonance of domain wall oscillations (DWR) has been reported in the FMR experiments in garnet thin films [16, 17]. This mode is excited by the r.f. field component parallel to magnetization within the domain and can overlap with the FMR modes. An exhaustive review of FMR studies in high–Q films and hybridized FMR–DWR oscillations has been given by Vukadinovic [18].

In the low–Q magnetic films with perpendicular anisotropy the situation is more complex: below the critical thickness the material displays the in–plane orientation of magnetization, forming large in–plane domains separated by the Neel–type walls. Above a critical thickness these films reveal stripe domain pattern, which is referred to as "weak stripe domains", characterized by the presence of flux closure caps. The dynamic response to high frequency magnetic excitations of such low–Q magnetic thin films has been studied by FMR in hexagonal Co [19, 20], FePd [18, 21], $Co_2MnGa$ [12] and by zero-field microwave susceptibility in several magnetic alloys, e.g. CoNbZr [22], CoFeZr [23], CoFeB [24] CoZrTa [25], and permalloy [26].

These studies, involving micromagnetic calculations and comparison with the experimental results, have shown that a number of different FMR modes could be excited, depending on the respective orientations of the pumping field and the DC bias field enforcing stripe orientation [19–21, 27]. In the particular configuration of microwave field in plane of the sample and perpendicular to the DC bias field (denoted as configuration "X") the selective excitation of two kinds of FMR modes in Co thin films has been demonstrated by Ebels [19, 20]. One is the acoustic FMR mode originating from magnetization inside the domains and the second set consists of two resonance modes related with the flux closure caps (cap breathing mode) [19, 20]. Vukadinovic presented the extended model, calculating the theoretical in–plane FMR spectra from the frequency and magnetic field dependence of magnetic susceptibility. These calculations, applied to FePd films with Q=0.4, confirmed that in the "X" configuration, the FMR spectra are dominated by

the acoustic mode, having its continuation in the uniform mode above saturation [21].

The micromagnetic simulations of the domain structure presented in the previous section show that our samples (Q=0.58) display a similar weak stripe domain pattern as Co films (Q≈0.5) studied in [19, 20] and FePd films (Q=0.4) studied in [18, 21]. Our experimental configuration (microwave field in plane of the sample and always perpendicular to the DC bias field) corresponds to the configuration "X" in Ref. [19, 21] Therefore, by analogy to the line assignment presented by Ebels [19], we attribute the broad absorption signal that we systematically observe at low fields in the X–band and Q–band experiments to the unresolved spectrum of excitation modes of magnetic moments located in different regions of flux closure caps. The volume involved in flux closure caps in our $Mn_5Ge_3$ films is clearly larger than in case of hexagonal Co, resulting in a broad absorption, rather than clearly resolved two peaks reported in [19, 20]. A similar broad absorption signal was observed at low fields in the FMR experiments on thin films of Heusler alloy $Co_2MnGa$ with stripe domain structure [12]. It is interesting to note that this signal has not been reported in previous FMR studies on $Mn_5Ge_3$ thin films [8, 28], even though they present FMR results in the unsaturated state.

The second component of our FMR spectra presented in Fig. 6 (X–band experiment in 68 nm $Mn_5Ge_3$ film)– i.e. a narrow, well–resolved resonance line–is interpreted as the acoustic mode of resonance excitations inside the domains, in agreement with the Ebels and Vukadinovic models for the "X" pumping configuration. This assignment is supported by the interesting feature presented in Fig. 6: the FMR signal is observed only when sweeping the DC field down after reaching an out–of–plane saturation, and the resonance field corresponding to this line (9.3 kOe) coincides with the domain nucleation region on hysteresis loop in this sample (inset in the Fig. 2). The domain structure corresponding to the point D (shown in the Fig. 4) consists of a number of well–defined cylindrical domains with magnetization opposite to the external field. This result shows clearly that the observation of this resonance mode is conditioned by the onset of a stable structure of oppositely oriented domains. The acoustic mode corresponds to the situation where the magnetization in neighboring, oppositely magnetized domains rotates in phase, coupled via the surface charges. The "optical" FMR mode is not observed in the present experiment, since it requires pumping along the DC field direction ("Y" configuration in Ebels notation).

In case of the Q–band experiments the resonance fields are clearly higher than the sample saturation field in both configurations the DC magnetic field. The resonance takes place in magnetically saturated state, all spins are aligned in the DC field direction and this line can be unambiguously interpreted as the uniform precession mode. In order to derive the resonance equations, the commonly accepted free energy approach, developed originally by Smit and Beljers [13] and extended by Baselgia et al. [29], was used here. The anisotropic part of magnetic free energy density F includes the Zeeman energy, the demagnetizing energy and uniaxial $K_u$ anisotropy energy density: $F=-\vec{M}\vec{H}+(2\pi M^2-K_u)\cos^2\theta$. The resonant condition at a fixed microwave frequency $\omega$ is given by

$$\left(\frac{\omega}{\gamma}\right)^2 = \frac{1}{M^2}\left\{\frac{\partial^2 F}{\partial\theta^2}\left(\frac{1}{sin^2\theta}\frac{\partial^2 F}{\partial\phi^2}+\frac{cos\theta}{sin\theta}\frac{\partial F}{\partial\theta}\right) - \left(\frac{1}{sin\theta}\frac{\partial^2 F}{\partial\theta\partial\phi}+\frac{cos\theta}{sin^2\theta}\frac{\partial F}{\partial\phi}\right)^2\right\} \quad (1)$$

where $\theta$ and $\phi$ are the polar and azimuthal angle of magnetization, respectively. The $\theta$ is counted from the film normal. The resonance field is obtained by evaluating Eq.(1) at the equilibrium position of **M** ( $\partial F/\partial\theta=0$ and $\partial F/\partial\phi=0$) for a given orientation of **H**. When magnetic field is applied perpendicular or parallel to the film surface, the Eq.(1) is reduced to a simple form known as classical Kittel's FMR equations [30]:

$$\frac{\omega}{\gamma} = H_\perp - 4\pi M_S + \frac{2K_u}{M_S} \quad (2)$$

in case of magnetic field applied perpendicular to sample plane and

$$\left(\frac{\omega}{\gamma}\right)^2 = H_\parallel\left(H_\parallel + 4\pi M_S - \frac{2K_u}{M_S}\right) \quad (3)$$

in case of magnetic field applied in sample plane.

The physical quantities $H_\parallel$, $H_\perp$ are resonance field values in the respective configurations, $M_S$–saturation magnetization, $K_u$–uniaxial anisotropy constant. In case of 68 nm thick sample, the resonance field at 295 K was $H_\parallel$ = 11.1 kOe and $H_\perp$ = 14.4 kOe, whereas saturation magnetization $M_S$= 250 emu/cm$^3$. Using these values we can determine the anisotropy constant of $Mn_5Ge_3$ at 295 K to be: $K_u=11\cdot10^4$ erg/cm$^3$. This result is comparable with the value previously determined in bulk $Mn_5Ge_3$ samples ($30\cdot10^4$ erg/cm$^3$) [31]. The difference may be related to

TABLE I. Uniaxial anisotropy constant (erg/cm$^3$) as a function of temperature determined from the FMR Q–band experiment in a series of $Mn_5Ge_3$ films .

| Thickness [nm] | Temperature [K] | | | | |
|---|---|---|---|---|---|
| | 15 | 50 | 100 | 200 | 295 |
| 9 | $5.41\cdot10^6$ | $5.06\cdot10^6$ | $4.69\cdot10^6$ | $3.22\cdot10^6$ | $2.65\cdot10^4$ |
| 18 | $5.66\cdot10^6$ | $5.27\cdot10^6$ | $4.73\cdot10^6$ | $3.16\cdot10^6$ | $2.74\cdot10^4$ |
| 68 | | | | | $11\cdot10^4$ |
| Bulk | | | $4.2\cdot10^6$[a] | | $30\cdot10^4$ |

[a] From Ref. [31] at 77 K

the fact that these values refer to the temperature bordering the Curie point.

In the 9 nm and 18 nm thick films the uniform precession signal could be observed in the Q–band at all studied temperatures, making it possible to calculate the $K_u$ values as a function of temperature for these films, as shown in Table 1. The values obtained for the 9 nm and 18 nm films are very close to each other at all temperatures and almost identical to the reported value for bulk at 77 K [31]. The scatter of $K_u$ values observed at room temperature ist most probably related to the vicinity of the Curie point, as already mentioned.

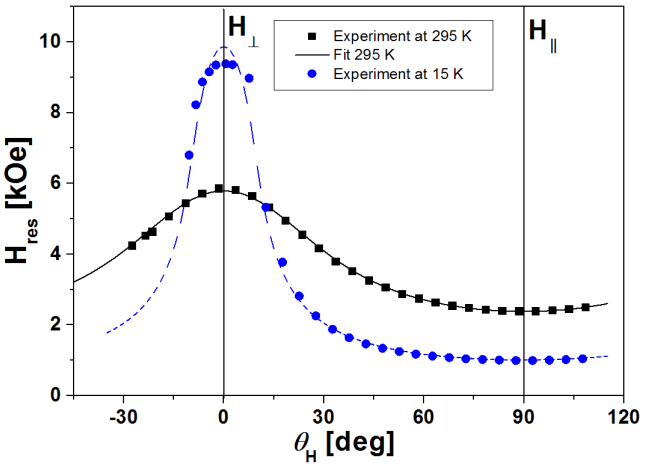


FIG. 9. (Color online) X–band FMR resonance field recorded in $Mn_5Ge_3$ film 68 nm thick at 15 K and 295 K as a function of angle between the external magnetic field and the film normal (0 deg.–field along normal, 90 deg.–field in sample plane). Blue dashed line for acoustic mode at 15 K serves as a guide to the eye. Solid black line at 295 K represents the fit as described in the text.

When rotating the DC magnetic field between the out–of–plane and in–plane direction of magnetic field one can trace the position of the acoustic mode, as shown in Fig. 9, where we plot the results of X–band experiments performed in 68 nm sample at 15 K and at 295 K. We note that at 295 K the position of resonance line is above saturation field in case of the in–plane orientation (H sat= 2 kOe) [32], and thus the observed resonance is the uniform precession mode. At the same time, for orientations close to the film normal the resonance field is still below saturation (H sat=7 kOe) [32] and the observed line is an acoustic mode. This is in line with the theoretical predictions that the acoustic mode transforms into uniform precession in the magnetically saturated state [20]. An attempt to fit the experimental data at 295 K using the Eq. (1), gave an excellent result for the following free parameters: $K_u$=9.1·10$^4$ erg/cm$^3$ and g–factor g=1.99. A slight difference between this result and the $K_u$ value obtained from the Q–band experiment (11·10$^4$ erg/cm$^3$) is attributed to the fact that in the out–of–plane configuration the sample is not fully saturated. Nevertheless, closeness of these values and the characteristic shape of the resonance field versus angle dependence confirm the correctness of our interpretation. In case of the data obtained at 15 K such fit would not have a physical meaning, since the Eq. (1) applies to the saturated state, and not to the acoustic mode. The solid line for the data at 15 K shown in Fig. 9 is only a guide to the eye, underlining the characteristic shape of the resonance field versus angle dependence.

The resonance field in the in–plane configuration of the acoustic mode is around 1 kOe at 15 K. The domain structure at this field is expected to resemble structures visualized in panel D in Fig. 3, i.e. domain magnetization is tilted in the field direction, and close to the surface it is oriented in plane. With decreasing film thickness the proportion of in–plane oriented moments increases, as revealed by the huge intensity of the broad absorption line (see Fig. 5), but the acoustic mode is still traceable, even in films as thin as 4.5 nm.

## IV. CONCLUSION

Extensive X–band and Q–band FMR experiments have been carried out in the $Mn_5Ge_3$ epitaxial films with thicknesses varying between 4.5 and 68 nm. The FMR signals were recorded in the temperature range between 15 and 295 K, at different orientations of magnetic field with respect to the film plane. In parallel, we performed the micromagnetic calculations of the domain structure of a $Mn_5Ge_3$ film 30 nm thick as a function of the magnetic field applied in the film plane and perpendicular to it. The theoretically calculated magnetization curves are fully consistent with the experimental ones, proving the correctness of the simulated domain structure generated within the same model. Analysis of the experimental FMR spectra in the context of the theoreticaly simulated domain structure, made it possible to assign the observed resonance modes to particular fragments of the domain structure: on one hand magnetization precession inside the stripe domain gives rise to an acoustic FMR mode with well–defined resonance field. On the other hand, a relatively large volume of magnetization inside closure caps, gives rise to the broad absorption spectrum of unresolved FMR lines, observed at low fields. Our results show unambiguously that in the film thickness range above 18 nm the uniaxial anisotropy leads to the stripe domain structure with closure caps containing a significant fraction of magnetic moments, supporting the results reported in Ref. [5]. This conclusion negates the interpretation of FMR data in $Mn_5Ge_3$ films presented in Ref. [8], where the authors claim that magnetization is entirely oriented in the film plane, and interpret the acoustic resonance mode as the uniform FMR mode. Our results stress the importance of combining the analysis of the FMR modes observed in magnetically non saturated materials with micromagnetic calculations and simulations of a domain structure. The effective uniaxial anisotropy constant in 18 nm film was found to vary between 5.66·10$^6$ erg/cm$^3$ at 15 K to 4.73·10$^6$ erg/cm$^3$

at 100 K in perfect agreement with the reported values for the bulk material. The room temperature values of $K_u$ reveal a significant scatter which is attributed to the vicinity of the Curie point.


[1] R. P. Panguluri, Ch. Zeng, H. H. Weitering, J. M. Sullivan, S. C. Erwin, and B. Nadgorny, Phys. Status Solidi B **242**, R67 (2005).

[2] I. Slipukhina, E. Arras, Ph. Mavropoulos, and P. Pochet, Appl. Phys. Lett. **94**, 192505 (2009).

[3] Ch. Zeng, S. C. Erwin, L. C. Feldman, A. P. Li, R. Jin, Y. Song, J. R. Thompson, and H. H. Weitering, Appl. Phys. Lett. **83**, 5002 (2003).

[4] Ch. Zeng, W. Zhu, S. C. Erwin, Z. Zhang, and H. H. Weitering, Phys. Rev. B **70**, 205340 (2004).

[5] A. Spiesser, F. Virot, L. A. Michez, R. Hayn, S. Bertaina, L. Favre, M. Petit, and V. Le Thanh, Phys. Rev. B **86**, 035211 (2012).

[6] S. Olive-Mendez, A. Spiesser, L. A. Michez, V. Le Thanh, A. Glachant, J. Derrien, T. Devillers, A. Barski, and M. Jamet, Thin Solid Films **517**, 191 (2008).

[7] L. A. Michez, A. Spiesser, M. Petit, S. Bertaina, J. F. Jacquot, D. Dufeu, C. Coudreau, M. Jamet, and V. Le Thanh, J. Phys–Condens. Mat. **27**, 266001 (2015).

[8] A. Truong, A. O. Watanabe, T. Sekiguchi, P. A. Mortemousque, T. Sato, K. Ando, and K. M. Itoh, Phys. Rev. B **90**, 224415 (2014).

[9] `http://math.nist.gov/oommf/`.

[10] M. Petit, L. Michez, Ch. E. Dutoit, S. Bertaina, V. O. Dolocan, V. Heresanu, M. Stoffel, and V. Le Thanh, Thin Solid Films **589**, 427 (2015).

[11] M. Hehn, S. Padovani, K. Ounadjela, and J. P. Bucher, Phys. Rev. B **54**, 3428 (1996).

[12] Ch. Yu, M. J. Pechan, D. Carr, and C. J. Palmstrom, J. Appl. Phys. **99**, 08J109 (2006).

[13] J. Smit and H. G. Beljers, Philips Res. Rep. **10**, 113 (1955).

[14] J. O. Artman and S. H. Charap, J. Appl. Phys. **49**, 1587 (1978).

[15] N. Vukadinovic, J. Ben Youssef, and H. Le Gall, J. Magn. Magn. Mater. **150**, 213 (1995).

[16] M. Ramesh, E. Jedryka, and P. E. Wigen, J. Appl. Phys. **57**, 3701 (1985).

[17] B. Luhrmann, H. Dotsch, and S. Sure, Appl. Phys. A **57**, 553 (1993).

[18] N. Vukadinovic, H. Le Gall, J. Ben Youssef, V. Gehanno, A. Marty, Y. Samson, and B. Gilles, Eur. Phys. J. B **13**, 445 (2000).

[19] U. Ebels, P. E. Wigen, and K. Ounadjela, Europhys. Lett. **46**, 94 (1999).

[20] U. Ebels, L. Buda, K. Ounadjela, and P. E. Wigen, Phys. Rev. B **63**, 174437 (2001).

[21] N. Vukadinovic, M. Labrune, J. Ben Youssef, A. Marty, J. C. Toussaint, and H. Le Gall, Phys. Rev. B **65**, 054403 (2001).

[22] Y. Shimada, M. Shimoda, and O. Kitakami, Jpn. J. Appl. Phys. **34**, 4786 (1995).

[23] O. Acher, C. Boscher, B. Brule, G. Perrin, N. Vukadinovic, G. Suran, and H. Joisten, J. Appl. Phys. **81**, 4057 (1997).

[24] C. Hengst, M. Wolf, R. Schafer, L. Schultz, and J. McCord, Phys. Rev. B **89**, 214412 (2014).

[25] U. Queitsch, J. McCord, A. Neudert, R. Schafer, L. Schultz, K. Rott, and H. Bruckl, J. Appl. Phys **100**, 093911 (2006).

[26] J. Ben Youssef, N. Vukadinovic, D. Billet, and M. Labrune, Phys. Rev. B **69**, 174402 (2004).

[27] N. Vukadinovic, O. Vacus, M. Labrune, O. Acher, and D. Pain, Phys. Rev. Lett. **85**, 2817 (2000).

[28] Ch. E. Dutoit, V. O. Dolocan, M. Kuzmin, L. Michez, M. Petit, V. Le Thanh, B. Pigeau, and S. Bertaina, J. Phys. D: Appl. Phys. **49**, 045001 (2016).

[29] L. Baselgia, M. Warden, F. Waldner, S. L. Hutton, J. E. Drumheller, Y. Q. He, P. E. Wigen, and M. Marysko, Phys. Rev. B **38**, 2237 (1988).

[30] C. Kittel, Phys. Rev. **73**, 155 (1948).

[31] Y. Tawara and K. Sato, J. Phys. Soc. Jpn. **18**, 773 (1963).

[32] L. A. Michez, F. Virot, M. Petit, R. Hayn, L. Notin, O. Fruchart, V. Heresanu, M. Jamet, and V. Le Thanh, J. Appl. Phys **118**, 043906 (2015).